Impedance-based Health Monitoring of Electromagnetic Coil Insulation Subjected to Corrosive Deterioration

N. Jordan Jameson[1], Michael H. Azarian[2], and Michael Pecht[3]

[1,2,3] *Center for Advanced Life Cycle Engineering, University of Maryland, College Park, MD, 20742, USA*
jjameson@umd.edu
mazarian@calce.umd.edu
pecht@calce.umd.edu

Abstract

Electromagnetic coils are widely used components in a variety of industries and systems, and their failure can lead to catastrophic failure of the system in which they are placed. Past studies have revealed the electromagnetic coil insulation to be a weakness, and there are presently no available methods to detect degradation in the coil insulation *in-situ*. Prior work in the AC motor community on twisted pairs of magnet wire has shown that insulation capacitance measurements can reveal useful diagnostic information. Yet, no studies have tracked the coil impedance spectrum over an aging/degradation period, no methods are available to identify frequencies in the impedance spectrum to be used, nor is there discussion concerning methods to employ coil impedance to determine a degradation mechanism. This paper develops an approach of detection of the aging of insulation in low-voltage electromagnetic coils when subjected to corrosive environmental conditions by assessing changes in impedance responses. The complex impedance was resolved into its real and imaginary parts and the Spearman correlation coefficient was used to find regions of interest within the impedance spectrum. The results indicate that real and imaginary impedance provide information that can assist in condition-based maintenance procedures for electromagnetic coils. Furthermore, by incorporating frequency-correlation analysis, the individual frequencies which provide diagnostic and prognostic information can be identified.

1. Introduction

Electromagnetic coils are fundamental components of many electromechanical systems. They are widely used in many industrial applications including motors, solenoids, and transformers. In solenoid-operated valves (SOVs), electromagnetic coils have been shown to cause a significant proportion of failures, as evidenced by a study conducted by Oak Ridge National Laboratory (Bacanskas, Roberts, & Toman, 1987) showing that over 50% of solenoid valve failures in U.S. nuclear power plants were attributed to electromagnetic coil faults (e.g., coil open, coil short). Moreover, solenoid-operated valves are often applied in safety-instrumented functions (SIFs), which, in general, preclude any health-monitoring activities involving valve actuation. In motors, electromagnetic coil insulation problems contribute to about one third of all motor failures (Thorsen & Dalva, 1995; Motor Reliability Working Group, 1985a, 1985b). Degradation of electromagnetic coil insulation can lead to failure of the coil and subsequently, the component and system in which the coil is used.

In a 2009 study, Angadi *et al*. (Angadi et al., 2009a, 2009b) performed accelerated testing of SOVs and concluded that the coils are susceptible to "coupled electrical-thermal-mechanical failure mechanisms," wherein the application of voltage causes Joule heating of the conductor wire, thus subjecting the insulation to thermal stresses from the temperature rise and mechanical stresses from the expansion of the conductor. These studies help indicate the insulation as a weak point in the electromagnetic coil. As a result, there is a need for methods to perform diagnostics and prognostics to enable condition-based maintenance and replacement of the electromagnetic coils prior to development of a fault that could cause catastrophic damage.

2. Prior Work

There has been much work addressing the problem of insulation health monitoring in machinery. In 2004, Stone *et al*. (Stone, Boulter, Culbert, & Dhirani, 2004) released a book that is a standard reference for insulation used in rotating machinery. In the book, the available methods of diagnostics for insulation were discussed. These methods include the measurement of the dissipation factor, insulation capacitance, polarization index, insulation resistance, insulation power factor, and offline partial discharge. A common necessity for the methods discussed is direct access to the insulation. The same requirement of direct access to the insulation exists for all methods presented in this book, except online partial discharge testing, which is only applicable to high-voltage (generally > 2.3kV) machines. For a system like the SOV (which generally operates in 120VAC or < 30VDC), and other low voltage machines, partial discharge monitoring is infeasible.

Others have investigated the use of coil impedance monitoring in insulation diagnostics (Werynski, Roger, Corton, & Brudny, 2006; Perisse, Werynski, & Roger, 2007; Perisse, Mercier, Lefevre, & Roger, 2009), not relying on direct access to the coil insulation. However, these proposed methods and their associated studies have not provided a full accounting for the evolution of the impedance spectrum over an aging/degradation period. Further it should be clear that as a polymeric material, the insulation will degrade in different manners when subjected to different loading conditions. When subjected to elevated temperatures, polymers will generally oxidize, leading to shortened molecular chains and decreased dielectric properties (Scheirs, 2000). When exposed to a moisture-rich environment, polymers can succumb to hydrolysis, which will also shorten the molecular chains, but in addition, will cause the capacitance to increase due to the diffusion of water into the insulation.

It is reasonable to assume that measuring the impedance spectrum of the electromagnetic coil will yield results that can be leveraged in a health-monitoring capacity, due to the distributed capacitance of the insulation (Massarini & Kazimierczuk, 1997; Grandi, Kazimierczuk, Massarini, & Reggiani, 1999). However, in order for impedance monitoring to be adopted, a general understanding of how the coil impedance spectrum evolves in various environmental conditions must be provided. Hence, this paper will present results from an experiment that illustrates the evolution of the impedance spectrum of an electromagnetic coil when exposed to an acidic environment, showing regions within the frequency spectrum that best correspond to the degradation, in order to provide insight into insulation degradation and approaches to its online measurement using coil impedance.

3. EXPERIMENTAL SETUP

This experiment is meant to test the capability of impedance measurements as a diagnostic tool for an electromagnetic coil. The coil used was hand-wound using AWG38 magnet wire coated with a polyester-imide based enamel. The conductor diameter was ≈ 180 μm and the insulation was ≈ 7.5 μm thick.

A sulfuric acid solution was used to accelerate the degradation. This decision followed the exposure of different pieces of the magnet wire to various compounds in order to find a degrading agent that operated on a time scale slow enough to measure changes in the impedance spectrum, but quick enough to degrade the insulation and demonstrate the efficacy of the impedance spectrum. A 50% distilled water-50% sulfuric acid (98% concentrated) solution degraded portions of the insulation within approximately a week and was chosen to serve as the degrading agent for the experiment.

The sulfuric acid solution was dripped onto the electromagnetic coil using a glass dropper, and each application was at the same location. During this process, the coil was connected to an Agilent E9080A LCR (inductance-capacitance-resistance) meter, which is capable of taking impedance measurements at frequencies ranging from 20Hz to 2MHz. The connection was made using the Agilent 16047E four-terminal fixture. The LCR meter was controlled externally using LabVIEW, programmed to measure impedance at 501 distinct frequencies over the entire operational range of the LCR meter, equally spaced in the base-10 logarithmic domain, with an RMS voltage of 500mV. The measurement time varied according to the frequency from 220-480 ms. At each frequency, 6 impedance measurements were taken sequentially and averaged to produce one final output measurement. Figure 1 shows the hand-wound coil, the connection between the coil and the LCR meter, and the location where the sulfuric acid solution was applied to the coil.

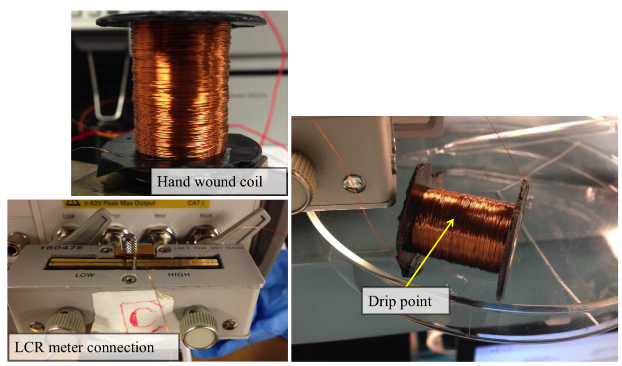

Figure 1. Test and measurement setup for acidic degradation experiment

The degradation impedance data can be represented as:

$$\mathbf{t} = \begin{bmatrix} t_0 & t_1 & \cdots & t_T \end{bmatrix}$$
$$\mathbf{Z} = \begin{bmatrix} Z(t_0, f_1) & Z(t_1, f_1) & \cdots & Z(t_T, f_1) \\ Z(t_0, f_2) & Z(t_1, f_2) & \cdots & Z(t_T, f_2) \\ \vdots & \vdots & \ddots & \vdots \\ Z(t_0, f_N) & Z(t_1, f_N) & \cdots & Z(t_T, f_N) \end{bmatrix} \quad (1)$$

In this experiment, $N = 501$ ($f_{501} = 2$MHz) and $T = 813$ ($t_{813} \approx 143$ hours). Some analysis methods are discussed in the next section.

4. ANALYSIS METHODS

The windings of an electromagnetic coil have a distributed capacitance associated with the insulation on the magnet wire (Massarini & Kazimierczuk, 1997; Grandi et al., 1999). Further, the insulation has a conductance associated with the material and any contaminants in the material (Younsi et al., 2010). The insulation capacitance and resistance will be captured in the measurement of coil impedance. Electrical impedance is a generalization of the opposition to current and is measured in Ohms (Ω). It is complex-valued and dependent upon frequency (ω), and can be expressed as: $Z(\omega) = R(\omega) + jX(\omega)$, where $j = \sqrt{-1}$ is the imaginary unit. The real part is called "resistance" and the imaginary part is called "reactance". Resistance is the opposition to electrical current, and reactance is the opposition to a change in voltage or current due to capacitive or inductive behavior. The impedance of an ideal resistor is purely real (R), while the impedance of an ideal inductor ($j\omega L$) or capacitor $\left((j\omega C)^{-1}\right)$ is purely imaginary. Positive reactance is referred to as "inductive reactance", while negative reactance is referred to as "capacitive reactance". The resonance of an electrical circuit is the frequency, ω_r, at which inductive reactance is exactly balanced by capacitive reactance, i.e., $X_L(\omega_r) + X_C(\omega_r) = 0$.

When searching for a health indicator to be used in a diagnostic or prognostic application, a desirable trait is for the health indicator to trend monotonically over the specified lifetime of the component or system. The Spearman rank correlation coefficient is a non-parametric measure of the monotonic relationship between two variables and can be employed to discover features useful for health monitoring. Essentially, the Spearman correlation coefficient is computed in the same manner as the Pearson correlation coefficient, except the raw data is first transformed into rankings. For a dataset of size n and where each point is distinct and non-repeated, the Spearman rank correlation coefficient is calculated as:

$$\rho = 1 - \frac{6}{n(n^2-1)} \sum_{i=1}^{n} d_i^2 \tag{2}$$

In this computation, the raw samples, X_i, Y_i, are converted into ranks x_i, y_i and $d_i = x_i - y_i$ is the distance between the ranks. Identical values (rank ties or value duplicates) are assigned a rank equal to the average of their positions in the ascending order of the values. The Spearman correlation coefficient ranges from $+1$ to -1 such that when $\rho = +1\,(-1)$, each of the variables is a perfect monotone increasing (decreasing) function of the other. The Spearman correlation coefficient can be used to measure linear or nonlinear monotonic relationships between two variables (Gautheir, 2001). The measure is more general than the Pearson correlation coefficient, which measures only linear dependence, whereas the Spearman correlation coefficient is invariant under monotonic transforms of the variables (Ekström, 2011). Further, the Spearman rank correlation coefficient does not operate under an assumption of normality in the variables. An example illustrating the Spearman correlation coefficient and the Pearson correlation coefficient is shown in Figure 2. For the example shown, assuming the variable y was indicative of system or component health, using the Spearman rank correlation coefficient provides a stronger indication that the feature indicated by the variable x, could serve as a health indicator.

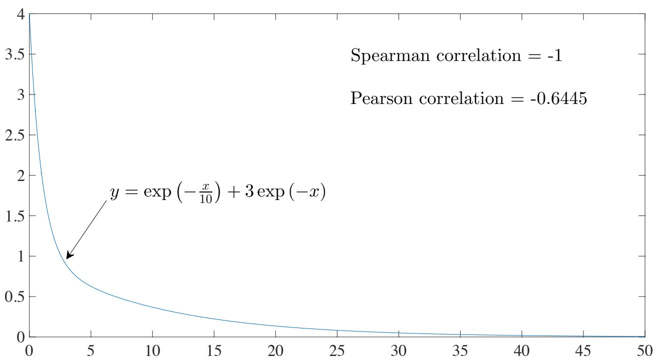

Figure 2. Pearson and Spearman correlation analysis for a nonlinear function $y = \exp(-x/10) + 3\exp(-x)$.

5. EXPERIMENTAL RESULTS

The time evolution of the impedance spectrum response to the sulfuric acid solution is shown in Figure 3. The application of the sulfuric acid solution caused an initial shift in the impedance spectrum that is likely due only to the presence of water and sulfuric acid (both of which have a higher permittivity than air) between the magnet wire turn-to-turn insulation, rather than true degradation of the magnet wire insulation. In the lower frequency portion of the resistance spectrum, there are several lines that appear to be outliers. These are sequential measurements (taken at $\approx$ 100 hours) and the result of incorrect connection of the coil magnet wire to the LCR meter. After the connection was corrected, the measurements resumed as expected. As the magnet wire insulation degraded, the resonant frequency shifted lower, and the resonant magnitude also decreased.

The Spearman correlation coefficient can be used to identify regions of the frequency spectrum that closely correspond to the exposure time. This is important when attempting to find a health indicator for diagnostics and prognostics. The Spearman correlation coefficient for all frequencies, separated for resistance and reactance, was calculated using the measurements at each frequency as a time series and then correlating these data with the time vector. Thus, the impedance at each frequency is assessed as a potential health indicator independently of the other frequencies. The noted outliers in the data were excluded from the correlation analysis.

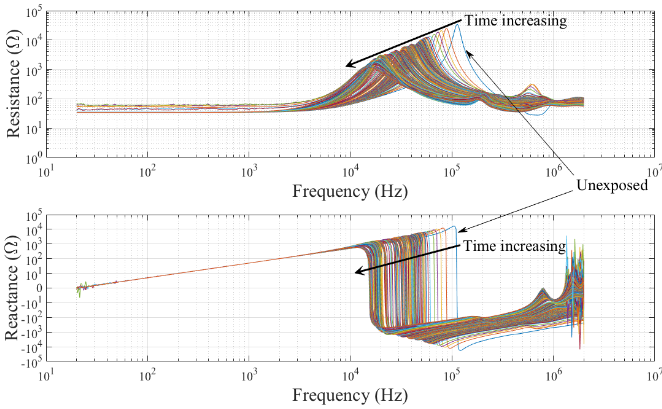

Figure 3. Evolution of the impedance spectrum due to sulfuric acid degradation over the total experiment time of $\approx$ 143 hours. The "Time increasing" arrow denotes the temporal progression of the impedance spectra (i.e., the first spectrum is the right-most curve).

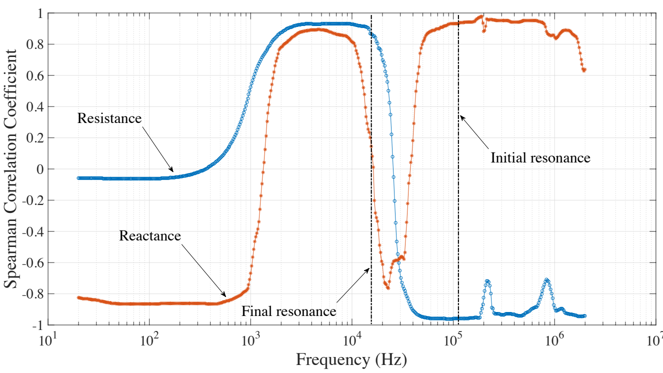

Figure 4. Spearman correlation coefficient computed according to Eq. 2 using the time series of impedance at each frequency and the overall time vector as variables (i.e., the time vector and each row of the impedance time-frequency matrix in Eq. 1). The erroneous data mentioned previously was not included in the correlation analysis.

Figure 4 shows the correlations of all frequencies with the total exposure time. The frequencies with highest correlations must be further investigated to understand the trends and find features to use for diagnostics and prognostics. However, some preliminary observations can be made. First, the resistance values at low frequencies show essentially no correlation with the exposure time, which implies that monitoring DC resistance would provide little indication of the developing faults in the insulation. Second, the entirety of capacitive reactance beyond $\approx$ 40 kHz is positively correlated with the exposure time. The resistance and reactance trends for some of the higher correlated frequencies are shown in Figures 5 and 6. The Spearman correlation coefficients for each frequency are shown in the figures. In the reactance figures, the mathematical expressions of inductive and capacitive reactance are shown. From these equations, it can be seen that the coil capacitance and the coil inductance increase for the frequencies shown.

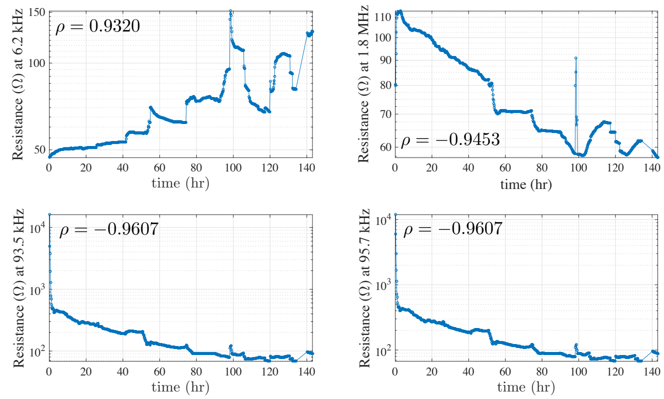

Figure 5. Resistance time series resulting from acidic degradation at (clockwise from upper left to lower left): 6.2 kHz; 1.8 MHz; 95.7 kHz; 93.5 kHz.

In the two lower plots for resistance in Figure 5, there is an initial steep increase, followed by a gradual decrease. This decrease continues for the remainder of the life of the insulation, though the rate of decrease slows. The two upper plots in Figure 6, shows that the coil capacitance increases over the degradation period. In both Figures 5 and 6, it can be observed that a significant jump in impedance occurred at $\approx$ 50 hour. The reason for this jump is hypothesized to be the exposure of a section of the magnet wire conductor, making the dielectric at this point purely the sulfuric acid solution, hence the jump in the capacitance, but slight decrease in resistance (due to conductivity of the solution).

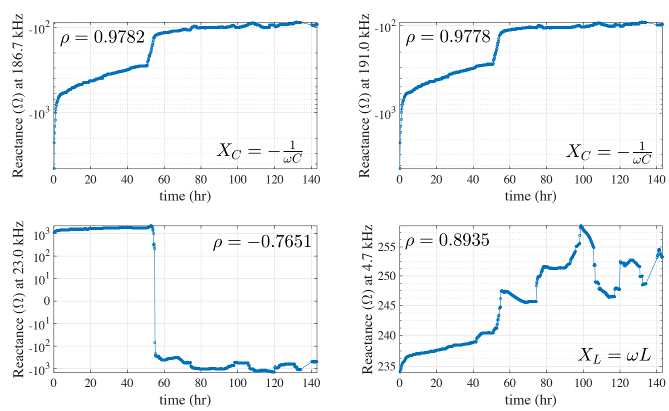

Figure 6. Reactance time series resulting from acidic degradation at (clockwise from upper left to lower left): 186.7 kHz; 191.0 kHz; 4.7 kHz; 23.0 kHz.

6. DISCUSSION

Consider the progression of the aging at frequencies just below (93-95 kHz) and just above (186-191 kHz) the original resonant impedance of the coil (which was at $\approx$ 112.5 kHz). At these frequencies, the degradation plots can approximately follow an exponential relationship (excluding the jump at ≈ 50 hr), which is expected with a first-order chemical rate phenomenon (Dakin, 1948). However, a better fit is provided with a sum of exponentials: one function prior to, and one function after, the hypothesized short formation at ≈ 50 hours, as shown in Figure 7.

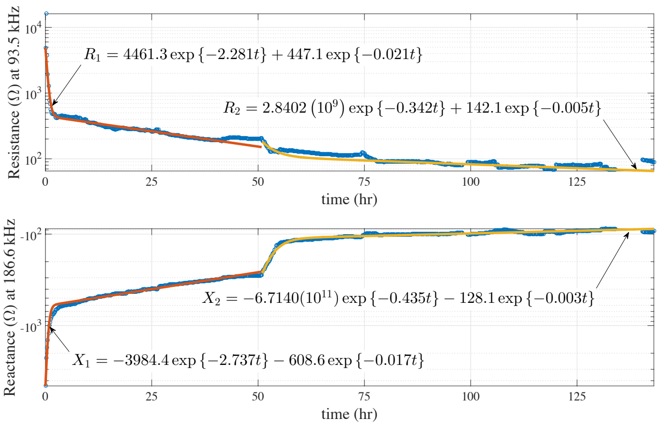

Figure 7. Data and sum of exponential functions fit for resistance at $f = 93.5$ kHz (fit with functions R_1 and R_2) and reactance at $f = 186.6$ kHz (fit with functions X_1 and X_2).

A sum of exponentials function is used to model the growth of a final product in set of three sequential first-order chemical reactions (i.e., $[A] \to [B] \to [C]$, where $[A]$ represents the concentration of chemical constituent A) (House, 2007, pp. 47-52). The curve fits shown in Figure 7 can thus be hypothesized to be a proxy measurement of the concentration of a product of two reactions (each a set of three sequential first-order reactions): one dominant until ≈ 50 hours and the other dominant beyond ≈ 50 hours. For region 1 ($t < 50.8$):

$$R_1(t) = 4461.3e^{-2.281t} + 447.1e^{-0.021t}$$
$$X_1(t) = -3984.4e^{-2.737t} - 608.6e^{-0.017t} \tag{3}$$

For region 2 ($t > 50.8$):

$$R_2(t) = 2.8402\left(10^9\right)e^{-0.342t} + 142.1e^{-0.005t}$$
$$X_2(t) = -6.7140\left(10^{11}\right)e^{-0.435t} - 128.1e^{-0.003t} \tag{4}$$

In each region the exponential decay terms are approximately equal for the resistance and reactance curves. From this analysis, it is reasonable to hypothesize that each region corresponds to a particular reaction involving three sequential first-order chemical reactions. The first region corresponds to the chemical degradation of the insulation from exposure to the sulfuric acid solution; the second region corresponds to the copper wire reacting with the sulfuric acid solution.

It is clear then that the impedance measurements at some frequencies reflect physical/chemical changes in the insulation that are occurring over the course of the experiment. Note that the capacitance changed by almost two orders of magnitude at frequencies just above resonant impedance (186-191kHz). Even before the jump in capacitance at ≈ 50 hr, the capacitance changed by about a factor of 10. This raises the question of the proper threshold for replacement of the coil. The threshold must be chosen such that useful life of the insulation is maximized, while prompting coil replacement prior to insulation failure in order to prevent catastrophic damage to the system in which the coil is used.

Perisse *et al.* (Perisse et al., 2009) suggested a criterion based on the resonant frequency, whereby the coil should be replaced when the resonant frequency dropped below 95% of the impedance resonant frequency. However, the resonant frequency for the coil in this experiment decreased by almost 72% before the formation of the first short. This information shows that the resonant impedance could shift by a much larger extent before the insulation fails. Thus, blindly replacing the coil after a 5% decrease in the resonant frequency would result in premature replacement of the coil and loss of useful insulation life. Electromagnetic coil insulation diagnostics and prognostics must then (at the very least) take in account both the degradation mechanism (in this case exposure to a corrosive substance) and the insulation material in order to truly assess the remaining useful life of the coil.

7. CONCLUSION

Insulation has been shown to be a major contributor to the failure of electromagnetic coils, especially those used in solenoid-operated valves (SOVs) and motors. Though there have been several attempts to develop methods for online insulation diagnostic and prognostic monitoring, the proposed methods have not adequately addressed the problem.

The ability of impedance from a low-level AC signal to detect degradation in electromagnetic coil insulation has been demonstrated in this paper. Using the Spearman correlation coefficient, the impedance spectrum, $Z(f)$, was probed for frequencies that provide health information. In the presented experiment, there are frequencies at which the impedance changed very little, and frequencies at which the impedance changed dramatically. The time series of resistance ($\Re\{Z(f)\}$) at $f = 93.5$ kHz and the reactance ($\Im\{Z(f)\}$) at $f = 186.6$ kHz were modeled using sum of exponentials functions. Separating the functions into two regions, prior to the formation of the short ($t < 50.8$) and after the formation of the short ($t > 50.8$), the exponential decay terms were similar (as shown in Eqns. 3 and 4), leading to the conclusion that these frequencies reflected chemical reactions occurring in the coil. Therefore, further diagnostic and prognostic efforts that use impedance measurements should focus on the relationship between the changing electrical properties of the insulation and the changing chemical properties of the insulation. Depending upon the application, the evolution of the mechanical properties of the insulation may also need to be tied to the electrical and chemical properties.

This research supports the goal of developing a diagnostic and prognostic model that can assist in condition-based maintenance and failure prevention of electromagnetic coils using knowledge of insulating materials and a baseline impedance spectrum. Further work is being pursued to understand the failure thresholds for different insulation materials when subjected to differing environmental conditions.

ACKNOWLEDGMENT

The authors would like to thank the more than 100 companies and organizations that support research activities at the Center for Advanced Life Cycle Engineering (CALCE) at the University of Maryland annually. Also special thanks go to the members of the Prognostics and Health Management Consortium at CALCE for their support of this work.

REFERENCES

Angadi, S., Jackson, R., Choe, S.-Y., Flowers, G., Suhling, J., Chang, Y.-K., & Ham, J.-K. (2009a). Reliability and life study of hydraulic solenoid valve. part 1: A multi-physics finite element model. *Engineering Failure Analysis*, *16*(3), 874–887.

Angadi, S., Jackson, R., Choe, S.-Y., Flowers, G., Suhling, J., Chang, Y.-K., … Bae, J.-i. (2009b). Reliability and life study of hydraulic solenoid valve. part 2: Experimental study. *Engineering Failure Analysis*, *16*(3), 944–963.

Bacanskas, V., Roberts, G., & Toman, G. (1987). *Aging and service wear of solenoid-operated valves used in safety systems of nuclear power plants, volume 1: Operating experience and failure identification* (Tech. Rep.). Franklin Research Center, Philadelphia, PA (USA); Oak Ridge National Lab., TN (USA); Nuclear Regulatory Commission, Washington, DC (USA).

Dakin, T. W. (1948). Electrical insulation deterioration treated as a chemical rate phenomenon. *Transactions of the American Institute of Electrical Engineers*, *67*(1), 113–122.

Ekström, J. (2011). On the relation between the polychoric correlation coefficient and spearman's rank correlation coefficient. *Department of Statistics, UCLA*.

Gautheir, T. D. (2001). Detecting trends using spearman's rank correlation coefficient. *Environmental forensics*, *2*(4), 359–362.

Grandi, G., Kazimierczuk, M. K., Massarini, A., & Reggiani, U. (1999). Stray capacitances of single-layer solenoid air-core inductors. *IEEE Transactions on Industry Applications*, *35*(5), 1162–1168.

House, J. E. (2007). *Principles of chemical kinetics*. Academic Press.

Massarini, A., & Kazimierczuk, M. K. (1997). Self-capacitance of inductors. *IEEE Transactions on Power Electronics*, *12*(4), 671–676.

Motor Reliability Working Group. (1985a, July). Report of large motor reliability survey of industrial and commercial installations, part 1. *IEEE Transactions on Industry Applications*, *IA-21*(4), 853-864. doi: 10.1109/TIA.1985.349532

Motor Reliability Working Group. (1985b, July). Report of large motor reliability survey of industrial and commercial installations, part 2. *IEEE Transactions on Industry Applications*, *IA-21*(4), 865-872. doi: 10.1109/TIA.1985.349533

Perisse, F., Mercier, D., Lefevre, E., & Roger, D. (2009). Robust diagnostics of stator insulation based on high frequency resonances measurements. *IEEE Transactions on Dielectrics and Electrical Insulation*, *16*(5), 1496–1502.

Perisse, F., Werynski, P., & Roger, D. (2007). A new method for ac machine turn insulation diagnostic based on high frequency resonances. *IEEE Transactions on Dielectrics and Electrical Insulation*, *14*(5), 1308–1315.

Scheirs, J. (2000). *Compositional and failure analysis of polymers: A practical approach*. John Wiley & Sons.

Stone, G. C., Boulter, E. A., Culbert, I., & Dhirani, H. (2004). *Electrical insulation for rotating machines: Design, evaluation, aging, testing, and repair*. John Wiley & Sons.

Thorsen, O. V., & Dalva, M. (1995). A survey of faults on induction motors in offshore oil industry, petrochemical industry, gas terminals, and oil refineries. *IEEE Transactions on Industry Applications*, *31*(5), 1186–1196.

Werynski, P., Roger, D., Corton, R., & Brudny, J. F. (2006). Proposition of a new method for in-service monitoring of the aging of stator winding insulation in ac motors. *IEEE Transactions on Energy Conversion*, *21*(3), 673–681.

Younsi, K., Neti, P., Shah, M., Zhou, J. Y., Krahn, J., Weeber, K., & Whitefield, C. D. (2010). On-line capacitance and dissipation factor monitoring of ac stator insulation. *IEEE Transactions on Dielectrics and Electrical Insulation*, *17*(5), 1441–1452.

BIOGRAPHIES

N. Jordan Jameson received the B.S. degree in mechanical engineering from Tennessee State University, Nashville, TN. He is currently a Ph.D. candidate in mechanical engineering at the University of Maryland, College Park. Jordan's research focuses on degradation mechanisms of electromagnetic coil insulation and methods to detect degraded insula-

tion prior to the formation of shorts in electromagnetic coils. Jordan has also worked in areas including conflict minerals in electronic systems, accelerated test methodologies for cooling pumps used in liquid cooling applications for servers, and the development of the IEEE Standard Framework for Prognosis and Health Management of Electronic Systems.

Michael H. Azarian received the B.S.E. degree in chemical engineering from Princeton University and the M.E. and Ph.D. degrees in materials science and engineering from Carnegie Mellon University. He is a Research Scientist with the Center for Advanced Life Cycle Engineering (CALCE), University of Maryland, College Park. Prior to joining CALCE he spent over 13 years in industry. His research focuses on the analysis, detection, prediction, and prevention of failures in electronic and electromechanical products. He is the holder of five U.S. patents. Dr. Azarian is co-chair of the Miscellaneous Techniques subcommittee of the SAE G-19A standards committee on detection of counterfeit parts. He has previously held leadership roles in various IEEE reliability standards committees and co-chaired iNEMI's Technology Working Group on Sensor Technology Roadmapping. He is on the Editorial Advisory Board of Soldering & Surface Mount Technology.

Michael Pecht received the M.S. degree in electrical engineering and the M.S. and Ph.D. degrees in engineering mechanics from the University of Wisconsin, Madison. He is the Founder of the Center for Advanced Life Cycle Engineering, University of Maryland, College Park, where he is also a George Dieter Chair Professor in mechanical engineering and a Professor in applied mathematics. He has consulted for over 100 major international electronics companies. He has written more than 20 books on electronic-product development, use, and supply chain management and over 400 technical articles. Dr. Pecht is a Professional Engineer and a fellow of ASME and IMAPS. He is the editor-in-chief of IEEE Access. He was the recipient of the IEEE Reliability Society's Lifetime Achievement Award, the European Micro and Nano-Reliability Award, the 3M Research Award for electronics packaging, and the IMAPS William D. Ashman Memorial Achievement Award for his contributions in electronics reliability analysis.